



A Robust Person Authentication System based on Score Level Fusion of Left and Right Irises and Retinal Features

L.Latha^{a,*}, S.Thangasamy^b

^aDepartment of Computer Science and Engineering, Kumaraguru College of Technology, Coimbatore-6, India

^bResearch & Development, Kumaraguru College of Technology, Coimbatore-6, India

Abstract

The recognition accuracy of a single biometric authentication system is often much reduced due to the environment, user mode and physiological defects. So a multimodal biometric approach for identity verification using two competent traits, iris and retina is proposed. This multimodal approach diminishes the drawback of single biometric system and improves the performance of an authentication system. Iris and Retina biometric recognition offers a highly reliable solution to person authentication. Iris recognition system is composed of segmentation, normalization, feature encoding and matching. Instead of using the entire iris code, only the bits that are consistent in the iris code called the Best bits are considered in the feature matching process. This reduces the computational time and storage requirements of iris code. To enhance the performance of recognition, the iris recognition process is applied to left and right irises separately and the corresponding distance scores are generated for each iris of a person. These scores are combined using the weighted sum fusion rule which further increases the recognition rate. In order to provide liveness verification for our authentication system, we also employed retinal blood vessel pattern recognition. This ensures the presence of only alive persons eliminating the possible spoofing attack. It is composed of segmentation, enhancement, feature encoding and matching. The scores from iris and retina recognition are then combined using weighted sum fusion rule, which further increases the recognition rate. To validate our approach, experiments were conducted on the iris and retina images obtained from CASIA and VARIA datasets respectively. A multimodal biometric database was constructed and then 1500 inter, intra image comparisons were made using the two datasets. The experimental results reveal that our multimodal biometric authentication system is much more reliable and precise than the single biometric approaches.

© 2010 Published by Elsevier Ltd. Open access under [CC BY-NC-ND license](https://creativecommons.org/licenses/by-nc-nd/4.0/).

Keywords: Best bits; Biometrics; Fusion; Iris; Matching score; Multimodal; Retina recognition; Weighted sum rule.

1. Introduction

Reliable automatic recognition of persons has long been an important and attractive goal of scientific research. In that sense, biometric authentication gets the leading role, since it cannot be borrowed, stolen or forgotten and forging is practically impossible. It is used as the most secure and convenient authentication tool. Biometric authentication provides an automated method of recognizing a person based on his physiological or behavioural characteristics. Various biometric systems have been developed based on fingerprints, facial features, voice, hand geometry, handwriting, retina, iris, etc. Multimodal biometric systems are those that utilize more than one physiological or behavioural characteristic for verification. It also provides anti-spoofing measures by making it difficult for an intruder to spoof multiple biometric traits simultaneously. By asking the user to present a random subset of biometric traits, the system ensures that a live user is indeed present at the point of acquisition. Iris recognition has received increasing attention in recent years as it provides promising solution to security issues [1] due to its uniqueness, stability and non-invasiveness. Iris is the annular part between the pupil and sclera in the human eye and it has an extraordinary texture, which is unique to each eye. Iris recognition process takes eye image as input and produces an output called iris code, which is the mathematical representation of the iris region in binary format. There are two types of bits in iris code. A bit in a subject's iris code is consistent if it assumes the same value for multiple images of that subject. The middle band

* Corresponding author.

E-mail address: surlatha@yahoo.com, latha.l.cse@kct.ac.in.

of iris code is more consistent than the outer and inner bands [2] and called as ‘best bits’. A bit is fragile if it varies in value for a substantial percent of the time. Not all the bits in an iris code are equally useful across different images of the same iris [2]. There are more number of inconsistent bits near the pupil and limbic boundary of the iris and can be masked. Possible causes of inconsistencies are due to improper segmentation, alignment issues and the coarse quantization of the phase response.

Retinal recognition is a relatively new approach, compared to other biometric features. Since retinal patterns have highly distinctive traits, the features extracted from retina identify effectively persons, even among genetically identical twins. Retinal vessel tree pattern has been proved to be a valid biometric trait for personal authentication as it is unique, time invariant and very hard to forge [3]. Retina is the light-sensitive layer of tissue that lines the inside of the eye and sends visual messages through the optic nerve to the brain. These vessels have a unique pattern that allows the generation of up to 400 data points for comparison. Retinal recognition technology captures and analyzes the patterns of blood vessels on the thin nerves that processes light entering through the pupil. A robust representation for retina recognition must be invariant to changes in size, position and orientation of the vessel patterns. The size of the actual template is only 96 bytes, which is very small by any standards. Thus, verification and identification processing times are much shorter than for other modalities. Liveness detection can also be provided by retina to thwart spoofing attacks at the sensor location. Liveness detection refers to the ability of the system to distinguish between a sample feature provided by a live human being and a copy of a feature provided by an artifact. Liveness of input retinal images is automatically ensured while authenticating in real-time, since the retinal pattern is visible only when the person is alive. It disappears when a person is no more.

The different biometric systems can be integrated at multi-modality level to improve the performance of verification system. A multimodal biometric system based on different traits is expected to be more robust to noise, address the problem of non-universality, improve the matching accuracy and provide reasonable protection against spoof attacks. Hence, the development of biometric systems based on multiple biometric traits has received considerable attention from researchers. In a multimodal biometric system that uses different biometric traits, various levels of fusion are possible: fusion at the feature extraction level, matching score level or decision level. It is difficult to consolidate information at the feature level because the feature sets used by different biometric modalities may either be inaccessible or incompatible. Fusion at the decision level is too rigid since only a limited amount of information is available at this level. Therefore, integration at the matching score level is generally preferred due to the ease in accessing and combining matching scores. Since the matching scores generated by the different modalities are heterogeneous, normalization is required to transform these scores into a common domain before combining them. The scores can then be combined into a single score and the final accept/reject decision is taken based on this score.

2. Related Works

Conventional Multimodal biometric systems operate at three levels; the feature level, the score level and the classifier level [4]. Until now, there has been little research into multi-unit iris recognition. In [5], a classifier level fusion method was proposed. This was a dynamic selection method that used one good quality iris image among the left and right iris images based on a quality checking pre-processing step. In other conventional iris systems, the researchers combined two pieces of information from the left and right iris images. However researchers only used

simple AND or OR rules in the classified levels. So, these approaches were simple and easy to implement, but the levels of accuracy were not sufficient compared to those achieved by score level fusion methods [4]. In [6], Daugman proposed modifications in his algorithm, including using active contour models for iris localization, handling off-axes gaze samples using Fourier-based methods, using statistical methods for detecting eyelashes and score normalization in large number databases. Sun et al. [7] proposed iris localization using texture segmentation. Huang et al. [8] used a noise removing approach based on the fusion of edge and region information. This method is specifically proposed for removing eyelash and pupil noises. Thornton et al. [9] used a general probabilistic framework for matching patterns of irises, which improves pattern-matching performance, when the iris tissue is subject to in-plane wrapping. Monro et al. in [10] present a novel iris coding algorithms based on differences of Discrete Cosine Transform (DCT) coefficients of overlapped angular patches with normalized iris image.

Marino et al. [11, 12] introduced an authentication system based on retina. The complete arterial–venous tree structure was used as the feature pattern for individuals. Based on the idea of fingerprint minutiae [13], a robust pattern was first introduced in [14], where a set of landmarks (bifurcations and crossovers of retinal vessel tree) were extracted and used as feature points. The database included only 6 individuals with 2 images for each of them. The drawback of the system was the necessity of storing and handling a whole image as the biometric pattern. [15] Describes a retinal verification method characterized by adding semantic information to the biometric pattern. It reduces the computation load in the matching process as only points classified equally can be matched. In [16,17] a pattern was defined using the optic disc as reference structure and using multi-scale analysis to compute a feature vector around it. The dataset size is 60 images, rotated 5 times each.

Ross and Jain [18] have presented an overview of Multimodal Biometrics and have proposed various levels of fusion, various possible scenarios, the different modes of operation, integration strategies and design issues. They have shown that the

combination approach performs better than some classification methods like decision tree and linear discriminant analysis. Apart from fusion of multi classifiers, much work has also been done to combine traits/modalities at various levels. Yunhong, et al. [19] proposed the fusion of iris and face modalities and reported that besides improving verification performance, the fusion of these two has several other advantages. Dass, et al. [20] have proposed an approach to score level fusion in multimodal biometrics systems. Common theoretical framework [21] for combining classifiers using sum rule, median rule, max and min rule are analyzed under the most restrictive assumptions and have observed that sum rule outperforms other classifiers combination schemes. The fusion methods include sum rule and product rule in rule-based fusion and support vector machines, multilayer perceptrons and binary decision trees in learning-based fusion. Research has shown that that the sum rule and support vector machines are generally superior to others [22, 23, 24]. The combined matching score can be computed as a weighted sum of the matching scores of the individual matchers [25, 26]. Kittler et al [27] have developed a theoretical framework for consolidating the evidence obtained from multiple classifiers using schemes like the sum rule, product rule, max rule, min rule, median rule and majority voting. In order to employ these schemes, the matching scores are converted into posteriori probabilities conforming to a genuine user and an impostor.

3. Iris Recognition System

The system is composed of a number of subsystems, which correspond to each stage of iris recognition. The stages include segmentation for locating the iris region in an eye image, normalization for creating a dimensionally consistent representation of the iris region, enhancement by histogram equalization of normalized iris region, feature encoding for creating an iris code containing only the most discriminating features of the iris and finally matching by hamming distance to make a decision of acceptance or rejection. The entire process is applied to both left and right irises separately. The two scores (hamming distances) calculated by the left and right irises are then combined to enhance the recognition rate.

3.1. Iris Segmentation

Segmentation is the first stage in iris preprocessing to isolate the actual iris region from a captured eye image. Canny method finds edges by looking for local maxima of the gradient of iris image. The gradient is calculated using the derivative of a Gaussian filter. It uses two thresholds to detect strong and weak edges. This method is more robust to noise and more likely to detect true weak edges. The output of the canny edge detector is the edge strength image and the orientation image. The image intensity value has to be increased by adjusting the gamma correction factor. With the orientation image and the adjusted gamma image as the input, the local maxima are suppressed.

3.2. Iris Normalization

Normalization is a process of transforming the segmented iris region into fixed dimension. However, dimensional inconsistencies arise between eye images due to the stretching of iris, caused by pupil dilation from varying levels of illumination. Such elastic deformation in iris texture will affect the result of iris matching. Therefore, normalization is done to compensate for iris deformation caused by illumination variations. This normalization process uses Daugman's rubber sheet model [28] and this method remaps the annular iris image $I(x, y)$ from raw Cartesian coordinates (x, y) to a dimensionless pseudo-polar coordinate system $I(r, \theta)$. Rubber sheet model takes into account the pupil dilation and size inconsistencies in order to produce a normalized representation with constant dimension. Normalization produces a 2D array with horizontal dimensions of angular resolution and vertical dimensions of radial resolution. A template of dimension 20 x 240 is produced, where 20 is the radial resolution and 240 is the angular resolution.

3.3. Iris Enhancement

Applying histogram equalization improves the contrast of the image by enhancing the normalized pattern. This method increases the global contrast of image, when the usable data of the image is represented by close contrast values. Through this adjustment, the intensities can be better distributed on the histogram. This allows for areas of lower local contrast to gain a higher contrast without affecting the global contrast. Histogram equalization accomplishes this effectively by spreading out the most frequent intensity values. The iris pattern before and after applying enhancement is shown in Fig 1.

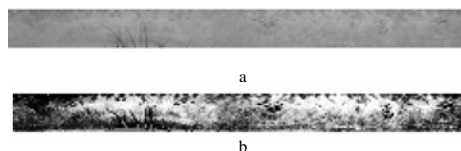


Fig. 1 a) Normalized image b) Enhanced image after histogram equalization

3.4 Feature Encoding

Feature encoding extracts the underlying information in an iris pattern and generates the binary iris template that is used in matching. Convolution of the normalized iris pattern with 1D Log-Gabor filter generates the iris feature set. The filter is Gaussian on a logarithmic scale and used to produce zero DC components for any bandwidth. It is given by

$$G(f) = \exp\left(\frac{-\log(f/f_0)^2}{2\log(\sigma/f_0)}\right) \quad (1)$$

where f_0 represents the centre frequency, and σ gives the bandwidth of the filter.

By applying 1D Log-Gabor filter, the 2D normalized pattern is divided into a number of 1D signals, and these are convolved with 1D Gabor wavelets. The rows of the 2D normalized pattern are taken as the 1D signal; each row corresponds to a circular ring on the iris region. The angular direction is taken, which corresponds to columns of the normalized pattern, since maximum independence occurs in the angular direction. The filter is constructed by calculating the radial filter component such as center frequency of filter and normalized radius from the center of frequency plane. The resultant complex features are phase quantized and encoded into binary iris templates [29].

3.5 Iris Matching

Matching is a process to determine whether two iris templates are from the same individual or not. Hamming distance is applied for bit-wise comparisons of images. Noise in the iris image is masked and only significant bits generated from the true iris region are used in the Hamming distance calculation between two iris templates [28].

$$HD = \frac{\|(\text{code } A \otimes \text{code } B) \cap (\text{mask } A \cap \text{mask } B)\|}{\|(\text{mask } A \cap \text{mask } B)\|} \quad (2)$$

where HD is the Hamming distance, A and B are two normalized iris images, code A and code B are the bit-codes of A and B, mask A and mask B are respectively the masks of noise of A and B. The hamming distance between the templates, which have deployed the best bits, is reduced compared to the use of full iris code.

4. Retina Recognition System

The proposed person authentication scheme contains four basic processes: segmentation, feature extraction, template generation and template matching. Segmentation process identifies the blood vessel pattern of the retina by using the oscillating components of scanning retinal images. The input image is projected onto a closed convex set [30] consisting of functions with zero mean. Then the signs of the projection are regarded as the output of the segmentation system. The method uses nonlinear orthogonal projection to capture the features of vessel network and a local adaptive threshold algorithm for vessel detection. This algorithm minimizes the vessel variation problem involved in image decomposition [31, 32]. The original retinal image and segmented vessel tree are shown in fig. 2(a) and fig. 2(b).

The vessel detection algorithm performs the following steps:

1. Compute the orthogonal projection using the fixed-point algorithm [30].
2. Apply threshold to the projection of step-1 to get the output binary image.
3. Apply morphological open operator to the binary image to remove blob-like structures and shorter linear structures.

4.1. Feature points Extraction

The features present in the retinal vessel tree are the bifurcations and crossovers, which are unique for every individual. The algorithm used here extracts these feature points called as retinal minutiae. As a preprocessing step, before extracting the features, thinning is performed and noise present in the scanned retinal image is filtered out. The blood vessels are thinned into one pixel width to find the bifurcation points accurately from the retinal images. First the boundary pixels of blood vessels are determined. A pixel is said to be a boundary pixel [33], if the pixel value is 0 and at least one of its four neighbors at horizontal and vertical pixel is 1. Then remove the boundary pixels that do not break the vessel connectivity. The resultant thinned image is shown in figure 3. Then Median filtering is used to decrease the false feature point detection rate by removing noisy pixels and bridging the gap between vessel lines. Due to eye movement during the image acquisition stage, patterns may suffer from deformations like translational, rotational displacements and non-linear distortion of blood vessels. To deal with these distortions of retinal patterns, first a minutiae-centered region is constructed to avoid the translation error. Then polar coordinate conversion

with respect to the corresponding core minutia is applied to handle the rotation distortion. Finally, tessellation quantification is performed to work with non-linear distortion by removing noise present in retina image.

The algorithm for feature extraction is given below:

1. Construct minutiae-centered region and represent each minutia as a 3-tuple $T(a,b,\theta)$ to avoid the translation error.
2. Transform step-1 into polar co-ordinate system to remove the rotation distortion and represent it as $T(\alpha, \beta, \gamma)$.
3. Apply tessellation quantification to step-2 to remove the non-linear distortion and get a rougher $T(rd,ra,o)$.
4. Perform steps 1 to 3 for all minutiae in retinal image and obtain the final feature template.

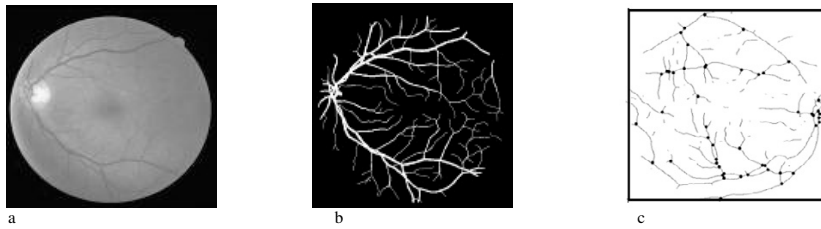


Fig.2 (a) Retinal image (b) Retinal vascular tree (c) Retinal template pattern

4.2. Template Creation and Matching

The blood vessel skeleton is removed from the input retinal image, by applying binary threshold after the process of extracting the bifurcation points. These bifurcation points are collectively stored in a template along with its coordinates. The generated template is shown in fig. 2(c). This process describes a methodology for verification of individuals based on retinal patterns. Since patterns may undergo translational or rotational displacements, it is necessary to align the images to be matched. The reference point detection method [34] is used to identify the blood vessel intersection points properly. The patterns compared could have a different number of points for the same individual, which is due to different conditions of illumination and orientation of the image in the acquisition process. Scaling is nearly constant for all images due to eye proximity to the camera. In addition, rotations are very slight as the eye orientation when facing the camera is very similar. Then matching of the intersection points is carried out. The number of matched blood vessel intersection points between the two patterns is used to quantify the degree of matching. This system generates a safe confidence band in the similarity measure space between scores for patterns of the same individual and between different individuals.

The template-matching algorithm is as follows:

Each retinal template is subdivided into 8×8 sized sub regions.

1. Let the two templates to be matched as TP1 and TP2 and sub regions as SR1 and SR2.
2. Initialize the total number of matched points in a template ‘TMP’ to be 0.
3. For each sub region SR1 in TP1 and SR2 in TP2 and for each intersection point IP1 in SR1, find the IP2 in SR2 and the 8 neighbor sub regions of SR2 which has minimum distance, D_{\min} with IP1. If $D_{\min} \leq D_{\text{thres}}$, distance threshold and IP2 are not already matched, then increment MP. Find TMP as $\text{TMP} + \text{MP}$.
4. Intersection points matching percentage is

$$P = (2 * \text{TMP} / (\text{TIP1} + \text{TIP2})) * 100 \quad (3)$$

where TIP1 is the total number of intersection points in TP1 and TIP2 is the total number of intersection points in TP2.

5. Similarity of matching is then given by

$$S = \max\{\text{Template Matching (TP1,TP2)}, \text{Template Matching (TP2, TP1)}\} \quad (4)$$

The distance threshold, D_{thres} represents the maximum offset by which, the same intersection point on different templates can be displaced. It is used in order to consider the quality loss and discontinuities arrived during the vessel extraction process that leads to dislocation of feature points by some pixels.

5. Fusion of iris and retina scores

Score level fusion of the hamming distances from the left and right irises is performed using weighted sum method. These techniques attempt to minimize the FRR for a given FAR. Once normalized, the scores from different modalities can be combined using simple operations such as max, min, sum or product. The sum and product rules allow for weighted combinations of scores. The weighting can be matcher specific, user specific [35] or based on sample quality. In matcher specific weighting, weights are chosen to be proportional to the accuracy of the matcher (e.g. inversely proportional to the Equal Error Rate for the matcher). In user specific weighting, weights are assigned based on how well the matcher is known to perform for a particular individual. Similarly, in quality based weighting, the weights are assigned based on quality of the sample (features) presented to the matcher. Although weighting techniques do offer performance improvements, the performance of simple sum and max fusion does not lag far behind. In addition these fusion methods do not require any training.

5.1. Fusion of distance scores from left and right irises

Sum rule fusion is a very promising multimodal biometrics fusion approach. The simplest form of combination would be to take the weighted average of the scores from the multiple units. This strategy was applied to all possible combinations of the two iris units. Equal weights were assigned to each unit. Given the matching scores of left iris and right iris, then the fused score is obtained by linearly combining the two scores as,

$$S_{Iris} = \frac{(1-\beta) \times S_{leftiris} + \beta \times S_{rightiris}}{2} \quad (5)$$

where β is a combination weight that can be computed using training data or made dependent on the quality of input. The set of weights that minimizes the total error rate (sum of the false accept and false reject rates) at some specified threshold is chosen. If more than one set of weights minimize the total error rate, then the set of weights that assigns almost equal weights to all the modalities is chosen. The threshold is set to a common value for users.

5.2. Fusion of distance and similarity scores from iris and retina

Since two different scores are obtained for iris and retina, score normalization needs to be performed in order to make the score range to lie within (0 to 1). So the z-score normalization is applied to the distance scores obtained from iris and similarity scores obtained from retina. In z-score normalization, the mean and standard deviation of the score vector S' are used to normalize the scores as shown in Eq. (6). The normalized score vector will have a mean of 0 and a standard deviation of 1:

$$S = (S' - \text{mean}(S')) / \text{std}(S') \quad (6)$$

Once the normalisation is done, then final score is obtained from the scores of fused iris unit and retina as,

$$S_{Final} = \frac{\alpha \times S_{Iris} + \beta \times S_{Retina}}{2} \quad (7)$$

where α and β represent the weights assigned to iris and retina traits of each user.

6. Experimental Results and Discussion

The reliability of the proposed multimodal biometric authentication system is described with the help of experimental results. The system has been tested using two different databases. CASIA [36] iris image database (version 3) created by National Laboratory of pattern recognition, Institute of Automation, Chinese Academy of Science is used for obtaining iris images. From this dataset, 500 left and 500 right iris image comparisons were made and the results were taken up for score level fusion later. Then 500 retinal images were taken from VARPA retinal images for authentication (VARIA) database [37] for constructing a multimodal database. The experiments were performed in Matlab 7.5. Comparisons of multiple biometric images of different persons generate inter user values and comparison of samples of the same person gives intra user values.

The performance measures used in our analysis are Genuine Acceptance Rate (GAR), False Acceptance Rate (FAR), False Rejection Rate (FRR) and Equal Error Rate (EER). The rate of accepting genuine user is called GAR and the rate of accepting imposter is called FAR. The rate of rejecting genuine user as an imposter is called FRR.

To obtain GAR, the extracted features of each person are compared with other image samples of the same person. In all the comparisons, if the similarity score is greater than the fixed threshold, then the person is accepted as a genuine user and if he is rejected, then it implies that a genuine person is not accepted i.e. falsely rejected. This gives FRR. To get FAR, the features of each person are compared with other persons' features in the database. In any of the comparisons, if the match score is more than the fixed threshold, then it implies that an imposter is accepted. Table 1 shows the set of values obtained for the above measures at different thresholds (Thr) for the iris database and Table 2 shows the set of values obtained for the retina dataset and the fusion of iris and retina scores.

Table 1. GAR, FAR and FRR rates at various thresholds for left and right irises and their fusion

Left Iris				Right Iris				Fusion by Sum Rule			
Thr	GAR in%	FAR in %	FRR in %	Thr	GAR in%	FAR in %	FRR in%	Thr	GAr in %	FAR in %	FRR in %
0.05	2.6	0.4	97.4	0.05	3.8	0	96.2	0.05	1.6	0	98.4
0.07	33.2	1.4	66.8	0.07	31.8	0	68.2	0.07	23	0	77
0.09	68.4	3.6	31.6	0.09	72.4	2	27.6	0.09	70	0.4	30
0.11	90.2	5.2	9.8	0.11	90.6	5.8	9.4	0.11	96.4	2.6	3.6
0.13	97	15.6	3	0.13	96.6	19	3.4	0.13	99.8	12.8	0.2
0.14	98	27.4	2	0.15	99.4	57.4	0.6	0.15	100	51.6	0
0.15	99.8	47.4	0.2	0.16	100	69.8	0	0.16	100	78	0
0.17	100	82	0	0.17	100	82.6	0	0.17	100	94.2	0
0.19	100	100	0	0.19	100	100	0	0.19	100	100	0

Table 2. GAR, FAR and FRR rates at various thresholds for Retina and fusion of Iris and Retina

Retina				Fusion of Iris and Retina			
Thr	GAR in%	FAR in %	FRR in %	Thr	GAR in%	FAR in %	FRR in%
20	100	0	100	0.35	20	1	79
25	100	0	98.9	0.4	32	2	67
30	100	0	72.1	0.45	49	3	50
40	82	17.9	0	0.55	79	12	20
45	39.5	60.4	0	0.6	89	21	10
50	6.69	93.3	0	0.65	94	38	5
60	4.31	95.6	0	0.7	97	50	2
65	2.37	97.6	0	0.75	98	65	1
80	2.37	97.6	0	0.85	99	89	0
90	2.37	97.6	0	1	100	100	0

ROC curve shows the measured accuracy performance of our biometric system. We have generated the ROC curves by varying the threshold on the classification image and an optimal threshold is selected as one that maximizes the accuracy. The ROC curve showing the relationship between GAR and FAR is shown in Fig 3. Equal Error Rate is the location on a ROC curve where FAR and FRR are equal. The EER is found from the ROC curve drawn between FAR and FRR as shown in Fig 4. The recognition rates are 90% and 88% with an EER of 0.051% and 0.06% for the left and right irises respectively. The score level fusion of distances from left and right irises yields a recognition rate of 96.4% and an EER of 0.025%. Thus the performance of multi-unit iris shows that there is a very good improvement in the recognition rate of multi unit system compared to the use of either left or right iris. Also the use of best bits reduces the computation time by nearly 50% and applying fusion methods reduce

the error rate further. The retinal authentication method gives 96.3% recognition rate and 0.015% EER. The proposed fusion of iris and retina increases the recognition rate to 99.3% and decreases the error rate to 0.01% which shows an enhanced performance by our system.

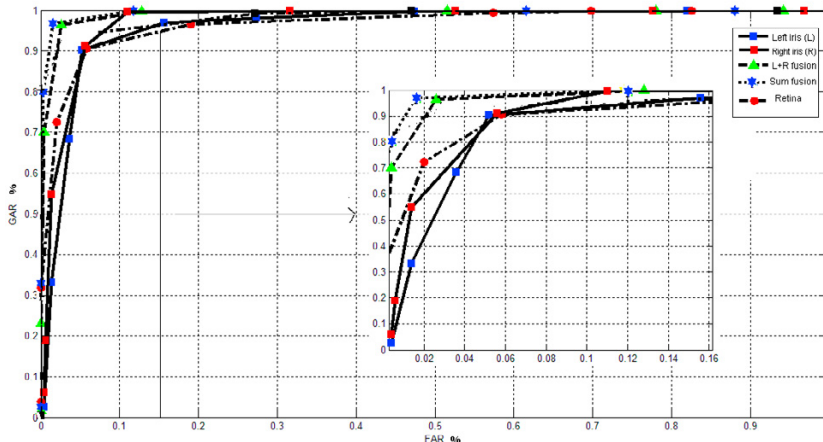


Fig. 3 ROC Curve between FAR and GAR for the two traits and their fusion

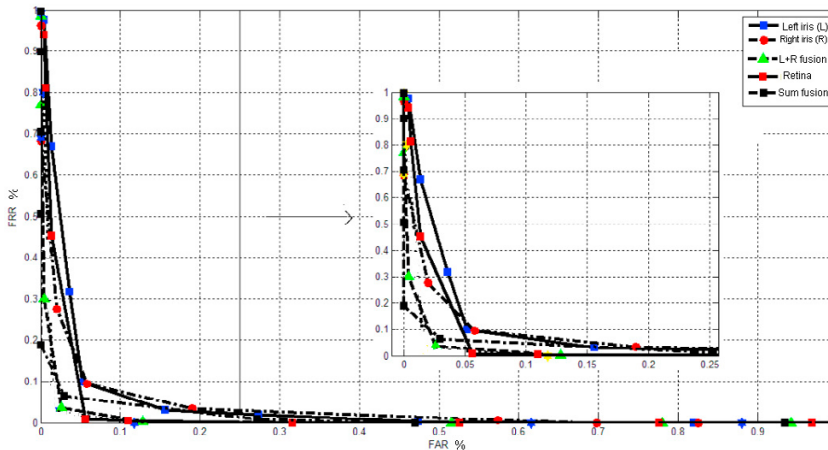


Fig. 4 ROC curve between FAR and FRR for the two traits and their fusion

7. Conclusion

Unimodal biometric systems fail in case of lack of proper biometric data for a particular trait. It is robust to use multiple biometrics for providing authentication. Thus the individual scores of two traits, iris and retina are combined at the matching score level to develop a multimodal biometric authentication system and it has been implemented in MATLAB. The method involves iris segmentation, generation of iris texture feature template and then matching by using the most consistent bits of the iris. This method reduces the feature set size and takes lesser processing time. The performance analysis is made using the publicly available CASIA database and the recognition rates are found to be 90% and 88% for left and right iris respectively. In order to improve the accuracy, a score level fusion of distances obtained from left and right irises is performed using weighted sum method. This shows a very good enhancement in the recognition rate to 96.4%, compared to the usage of left or right iris alone. Then person authentication by retinal pattern matching is performed that involves blood vessel segmentation, generation of feature template consisting of the bifurcation points and then matching of these points. The number of matched points in the compared templates quantifies the degree of matching. This method is quite insensitive to translational and rotational displacement of retinal images. In addition, the retinal template contains only the intersection points and not the entire vessel structure, so the storage requirement is less. The performance analysis is carried out by using the VARIA dataset and it gives 96.3% recognition rate. Finally, a good improvement in the performance is achieved by the fusion of iris and retina scores using weighted sum rule, which gives the recognition rate as 99.3%.

Acknowledgements

The authors wish to thank the National Laboratory of pattern recognition, Institute of Automation, Chinese Academy of Science, CASIA for providing the iris image database and VARPA retinal images for authentication, VARIA for providing retinal images.

References

- [1] P.Padma Polash and M. Maruf Monwar, "Human iris recognition for biometric identification", IEEE 10th international conference on Computer and information technology, pp. 1-5, 2007.
- [2] Karen P. Hollingsworth, Kevin W. Bowyer, Patrick J. Flynn, "The Best Bits in an Iris Code", IEEE Trans. Pattern Analysis and Machine Intelligence Vol. 31 no. 6, pp. 964-973, June 2009.
- [3] R.B.Hill, "Retinal identification, in Biometrics: Personal Identification in Networked Society", A.Jain, R.Bolle, and S.Pankati, Eds., p.126, Springer, Berlin, Germany, 1999.
- [4] Ross, A., Jain, A., Qian, J.Z., "Information fusion in biometrics", Pattern Recognit. Lett., vol. 24, no. 13, pp. 2115–2125, 2003.
- [5] Jain, J., Son, J., Lee, Y., Park, K.R., "Multi-unit iris recognition system by image check algorithm", Lecture Notes in Computer Science on ICBA2004, vol. 3072, pp. 450–457, 2004.
- [6] J. Daugman, "New methods in iris recognition", IEEE Transactions on Systems, Man, and Cybernetics, Part B, vol. 37, no. 5, pp. 1167–1175, 2007.
- [7] Z. Sun, Y. Wang, T. Tan, and J. Cui, "Improving iris recognition accuracy via cascaded classifiers", IEEE Transactions on Systems, Man and Cybernetics, Part C, vol. 35, no. 3, pp. 435–441, 2005.
- [8] J. Huang, L. Ma, T. Tan, and Y. Wang, "Learning based enhancement model of iris", Proceedings of the 14th British Machine Vision Conference (BMVC '03), pp. 153–162, Norwich, UK, September 2003.
- [9] J. Thornton, M. Savvides, and V. Kumar, "A Bayesian approach to deformed pattern matching of iris images", IEEE Transactions on Pattern Analysis and Machine Intelligence, vol. 29, no. 4, pp. 596–606, 2007.
- [10] D. M. Monro, S. Rakshit, and D. Zhang, "DCT-based iris recognition", IEEE Transactions on Pattern Analysis and Machine Intelligence, vol. 29, no. 4, pp. 586–595, 2007.
- [11] C.Marino, M.G.Penedo, M.Penas, M.J.Carreira, F.Gonzalez, "Personal authentication using digital retinal images", Pattern Analysis and Applications (2006) 9: 21–33.
- [12] C.Marino, M.G.Penedo, M.J.Carreira, F.Gonzalez, "Retinal angiography Based Authentication", Lecture Notes in Computer Science, vol.2905, Springer, Berlin, 2003, pp.306–313.
- [13] A. K. Jain, L. Hong, S. Pankanti, and R. Bolle, "An identity authentication system using fingerprints", Proceedings of the IEEE, vol. 85, no. 9, pp. 1365–1388, 1997.
- [14] M.Ortega, C.Marino, M.G. Penedo, M.Blanco, F.Gonzalez, "Biometric Authentication Using Digital Retinal Images", Proceedings of the 5th WSEAS International Conference on Applied Computer Science (ACOS 06), pp.422-427, Hangzhou, China, April 2006.
- [15] Marcos Ortega, M.G.Penedo, J.Rouco, N.Barreira, M.J.Carreira, "Personal verification based on extraction and characterization of retinal feature points", Journal of Visual Languages and Computing, pages 80-90, 2009.
- [16] H. Farzin, H. Abrishami-Moghaddam, and M.-S. Moin, "A novel retinal identification system", EURASIP Journal on Advances in Signal Processing, vol. 2008, Article ID 280635, 10 pages, 2008.
- [17] M. Ortega, C. Mariño, M. G. Penedo, M. Blanco, and F.González, "Personal authentication based on feature extraction and optic nerve location in digital retinal images", WSEAS Transactions on Computers, vol. 5, no. 6, pp. 1169–1176, 2006.
- [18] A. Ross & A. K. Jain, "Information Fusion in Biometrics", Pattern Recognition Letters, 24 (13), pp. 2115-2125, 2003.
- [19] W. Yunhong, T. Tan & A. K. Jain, "Combining Face and Iris Biometrics for Identity Verification", Proceedings of Fourth International Conference on AVBPA, pp. 805-813, 2003
- [20] S. C. Dass, K. Nandakumar & A. K. Jain, "A principal approach to score level fusion in Multimodal Biometrics System", Proceedings of ABVPA, 2005.
- [21] J. Kittler, M. Hatef, R. P. W. Duin, & J. Mates, "On combining classifiers", IEEE Transactions on Pattern Analysis and Machine Intelligence, 20(3), pp. 226–239, 1998.
- [22] J.J. Brault & R. Plamondon, "Segmenting Handwritten Signatures at Their Perceptually Important Points", IEEE Transactions on Pattern Analysis and Machine Intelligence, 15,
- [23] M. Ammar, T. Fukumura, & Y. Yoshida, "A new effective approach for off-line verification of signature by using pressure features", 8th International Conference on Pattern Recognition, pp. 566-569, 1986
- [24] M. A. Ismail, S. Gad, "Off-line Arabic signature recognition and verification", Pattern Recognition, 33 pp. 1727-1740, 2000
- [25] A. Ross, A.K. Jain, "Information fusion in biometrics", Pattern Recogn. Lett. 24 (13) (2003) 2115–2125 (special issue on multimodal biometrics).
- [26] Y. Wang, T. Tan, A.K. Jain, "Combining face and iris biometrics for identity verification", Proceedings of Fourth International Conference on AVBPA, Guildford, UK, 2003, pp. 805–813.
- [27] J. Kittler, M. Hatef, R.P. Duin, J.G. Matas, "On combining classifiers", IEEE Trans. Pattern Anal. Mach. Intell. 20 (3) (1998) 226–239.
- [28] J. Daugman, "How Iris Recognition Works", IEEE Trans. Circuits and Systems for Video Technology, Vol.14, no.1, pp.21-30, 2004
- [29] Amir Azizi, Hamid Reza Pourreza, "Efficient Iris Recognition through Improvement of Feature Extraction and subset Selection", International Journal of Computer Science and Information Security, Vol.2, No.1, 2009.

- [30] Yongping Zhang, Wynne Hsu, Mong Li Lee, "Detection of Retinal Blood Vessels Based on Nonlinear Projections", *Journal of Signal Processing Systems* (2009) 55:103-112.
- [31] Chambolle, A. (2004). "An algorithm for total variation minimization and applications", *Journal Mathematical Imaging and Vision*, 20, 89–97.
- [32] Aujol, J. F., Gilboa, G., Chan, T., & Osher, S. (2006). "Structure texture image decomposition—Modeling, algorithms, and parameter selection", *International Journal of Computer Vision*, 67(1), 111–136.
- [33] Rafael C. Gonzalez, Richard E. Woods, Steven L. Eddins (2004). *Digital Image Processing using MATLAB*. Prentice Hall.
- [34] Muhhamad Nazrul Islam, Md. Amran Siddiqui and Samiron Paul, "An Efficient Retina Pattern Recognition Algorithm (RPRA) towards Human Identification", 2nd International Conference on Computer, Control and Communication, IC4 2009, pp.1 – 6, 2009.
- [35] Snelick, R., Uludag, U., Mink, A., Indovina, M., Jain, A., 2005. "Large scale evaluation of multimodal biometric authentication using state-of-the-art systems", *IEEE Trans. Pattern Anal. Machine Intell.* (27), 450–455.
- [36] CASIA Iris Image Database, <http://www.sinobiometrics.com>, 2007.
- [37] VARIA, VARPA retinal images for authentication, <http://www.varpa.es/varia.html>